Sādhanā (2022) 47:212
https://doi.org/10.1007/s12046-022-01992-2

3D printed sensor for online condition monitoring of energy storage device

RUPINDER SINGH[1,*], ADESH GREWAL[2], AMRINDER PAL SINGH[2], VINAY KUMAR[3], MAHDI BODAGHI[4], AHMAD SERJOUEI[4] and YANG WEI[4]

[1]Department of Mechanical Engineering, NITTTR, Chandigarh, India
[2]Department of Mechanical Engineering, PU, Chandigarh, India
[3]Department of Mechanical and Production Engineering, GNDEC, Ludhiana, India
[4]Department of Engineering, NTU, Nottingham, UK
e-mail: rupindersingh@nitttrchd.ac.in

MS received 8 May 2022; revised 30 July 2022; accepted 8 September 2022

Abstract. In the past two decades' significant studies have been reported on electrically conducting thermoplastic composites of acrylonitrile butadiene styrene (ABS), polyvinylidene fluoride (PVDF), etc. for the fabrication of novel energy storage devices (ESD) by 3D printing. But hitherto little has been reported on online condition monitoring of ESD prepared by secondary (2°) recycling of ABS. This study reports the investigations on mechanical and electrical properties of NH_4Cl–$ZnCl_2$ (electrolyte) reinforced ABS composite (as 3D printed sensor) for online condition monitoring of ESD. In a typical dry cell, the electrolyte is one of the integral parts, and the change in its dielectric properties with the time/ applied electric load has been used to ascertain the health of ESD (online) as the internet of things (IoT) based solution (Bluetooth application) in industry sports and medicine (ISM) band (2.4 GHz). Based on melt flow index (MFI), 10% NH_4Cl and 10% $ZnCl_2$ (by weight%) were reinforced in ABS for preparing 3D printed rectangular substrates as ring resonators for calculating dielectric constant (ε_r) and loss tangent/dissipation factor (tanδ) for the resonant frequency. Transmission line parameters (S_{21}) were observed using a vector network analyzer (VNA), and a high-frequency structure simulation (HFSS) software package. The results are supported by morphological analysis of ABS composite based on scanning electron microscopy (SEM), energy dispersion spectroscopy (EDS), 3D rendering, surface roughness (R_a), area mapping, current (I)–voltage (V), and Fourier transformed infrared (FTIR) characterization.

Keywords. Acrylonitrile butadiene styrene; NH_4Cl–$ZnCl_2$; 3D printed substrate; I–V properties; FTIR.

1. Introduction

Thermoplastics like PVDF, polylactic acid (PLA), nylon 6, and ABS have wide engineering applications because of their high durability and cost-effectiveness. 3D printing of electrically conducting ABS-carbon black composite has been reported as a low-cost concave capacitor type polymeric sensor to measure the void fraction in a single and multi-component system in which two-phase flow takes place [1]. A highly conductive ABS-graphite-based electrochemical sensor for the detection of toxic gases has been prepared by a 3D printing process that highlights the industrial applications of ABS for sensor fabrication [2]. Some studies reported on circular ring-type patch antennas using conventional substrate materials like FR4, Roger, etc. for head imaging and 5G connectivity applications have also outlined the scope of thermoplastics for manufacturing cost-effective antennas [3, 4]. The review of the literature reported on antenna/ sensor designs and applications has outlined that 3D printable composites of polytetrafluoroethylene (PTFE)-glass fiber, PVDF-polypyrrole-carbon nanotubes, and dielectric tuned PLA may be used as sensors because such composites possess acceptable conductivity and transducer properties for sensor applications [5–8]. The role of composite, thermoplastics, thermosetting, and meta-materials has been observed as very useful in recent studies for the design and development of patch antenna structures for signal transmission and microwave applications [9–11]. Fused deposition modeling (FDM) based 3D printing of ABS, nylon, and bakelite-low density polyethylene composites have been explored as an effective tool to fabricate complex dielectric structures from such materials for sensing devices [12–14]. Various

*For correspondence
Published online: 26 October 2022

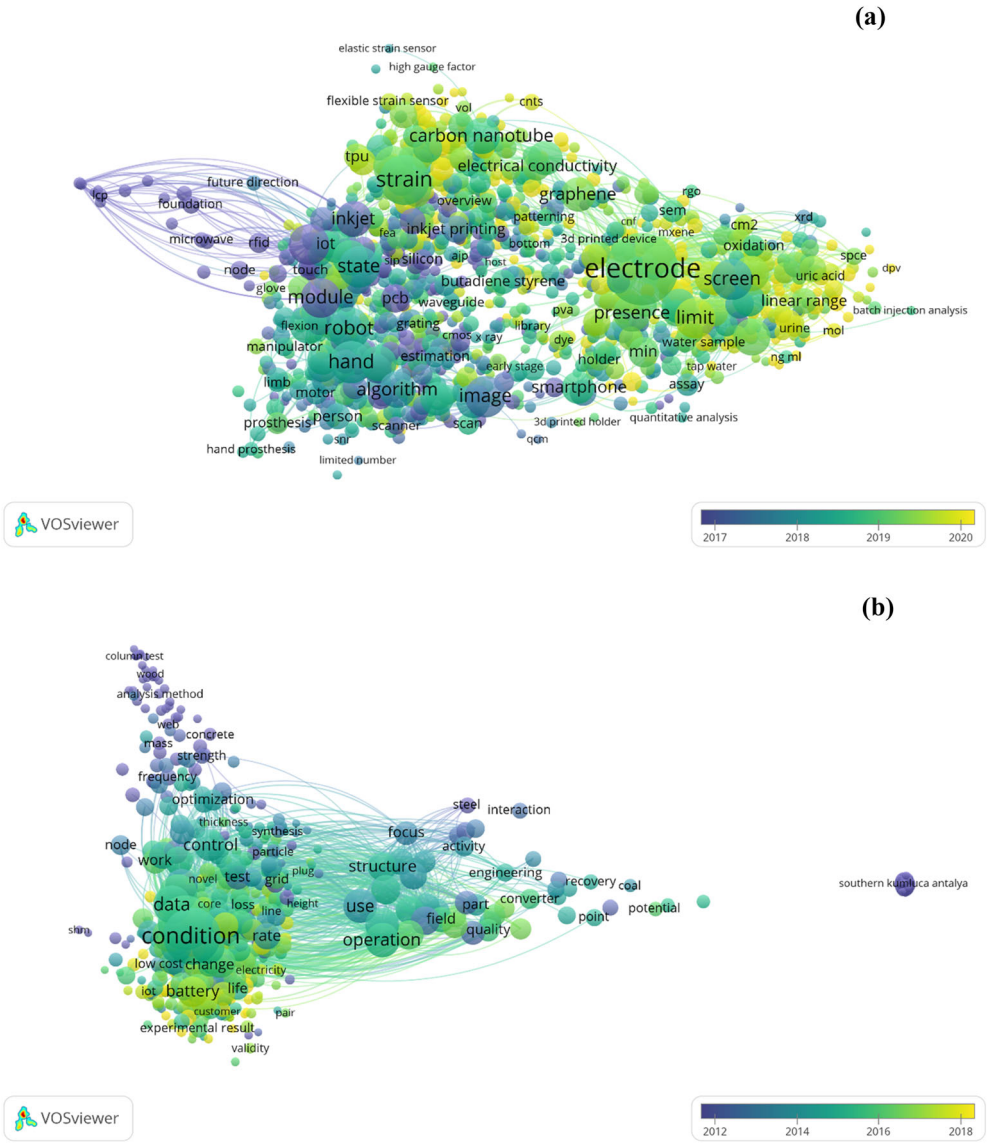

Figure 1. (**a**) Networking diagrams for keywords 3D printed sensors (**b**) 3D printed energy storage devices.

surveys performed on manufacturing practices have highlighted the issue of plastic waste generation at a large scale during traditional and non-traditional manufacturing of plastic goods. Recycling of plastic solid waste (like PLA, ABS, PVDF, etc.) by mechanical/chemical-assisted mechanical processing for 3D printing applications has been widely reported [15–18]. The 4D properties in ABS-based composite and industrial uses of NH_4Cl and $ZnCl_2$ electrolytes have been reported for energy harvesting in nano-power generator devices and ESD. This indicates that such materials may also be used as sensors to monitor the health of ESD prepared by 3D printing processes [19–23]. Some studies outlined that the functional prototypes of ABS and its electro-active composites fabricated by single or multi-material 3D printing processes outlined good mechanical, structural, thermal, and electrical properties in ABS for one-way programmable sensing applications [24–29].

To ascertain the research gap, Scopus database of the past 15 years was explored for keywords 3D printed sensors, 3D printed energy storage devices, and correspondingly 3168, 328 results were obtained. For 3D printed sensors, online condition monitoring, and energy storage device no work has been reported. The reported literature as per the Scopus database was processed using VOSviewer open-source software for bibliographic analysis. For 3D printed sensors (3168 results), 44298 repetitive terms were observed. By selecting No. of repetitions as '5' out of 44298 terms, 2159 met the threshold. For each of 2159 terms, a relevance score was calculated and 60% (1295) of

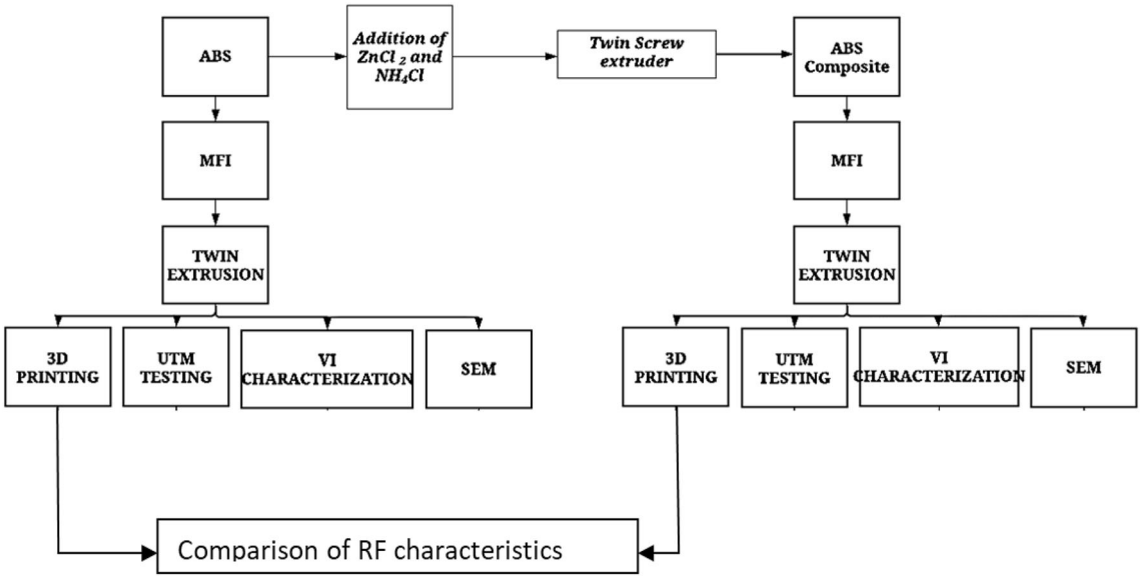

Figure 2. Work methodology for 3D printed sensors.

Table 1. Average MFI of 1° recycled ABS and 2° recycled ABS-NH_4Cl-$ZnCl_2$ composite.

Composition/proportion	MFI g/(10 min)
1° recycled ABS (100%)	15.31±0.03
90%ABS: 5%NH_4Cl: 5%$ZnCl_2$	6.37±0.04
80%ABS: 10%NH_4Cl: 10%$ZnCl_2$	3.89±0.03
70%ABS: 15%NH_4Cl: 15%$ZnCl_2$	1.07±0.04**

**Composition 70%ABS: 15%NH_4Cl: 15%$ZnCl_2$ was observed as non-useful for 3D printing due to the non-uniform flow of material (visual observation)

the most relevant terms were selected for further analysis. Similarly for keyword 3D printed energy storage devices, (328 results), 15314 repetitive terms were observed. By selecting No. of repetitions as '5' out of 15314 terms, 879 met the threshold. For each of 879 terms, a relevance score was calculated and 60% (527) of the most relevant terms were selected for further analysis. Figure 1a and b respectively show networking diagrams as bibliographic analysis for keywords 3D printed sensors and 3D printed energy storage devices.

Based on figure 1, it has been observed that little has been reported on online condition monitoring of ESD prepared by 2° recycling of ABS. This study reports the investigations on mechanical and electrical properties of electrolyte reinforced ABS composite (as 3D printed sensor) for online condition monitoring of ESD. In a typical dry cell, the electrolyte is one of the integral parts and the change in its dielectric properties with the time/applied electric load has been used to ascertain the health of ESD (online) as the IoT-based solution (Bluetooth application) in ISM band (2.45 GHz). Based on the MFI test, 10% NH_4Cl and 10% $ZnCl_2$ (by weight %) were reinforced in ABS for preparing 3D printed rectangular substrates of a ring resonator for calculating ε_r and tanδ (for the resonant frequency of 2.45 GHz). The S_{21} parameters were observed using a VNA, and HFSS software package.

2. Materials and method

For the present work, recycled ABS granules, and electrolytes (NH_4Cl, and $ZnCl_2$) were procured from a local market to fabricate 3D printed sensors. Rheological analysis based upon MFI was performed for ABS and mechanically blended ABS-NH_4Cl-$ZnCl_2$ composite as per ASTM D 1238. Further analysis of mechanical, and

Table 2. FDM process parameters for 3D printing of ABS and its composite.

Composition	Nozzle temperature (°C)	Bed temperature (°C)	Filament flow rate (mm/min)
1° Recycled ABS	220	90	60
2° Recycled ABS (ABS-10%NH_4Cl–10%$ZnCl_2$)	230	92	40

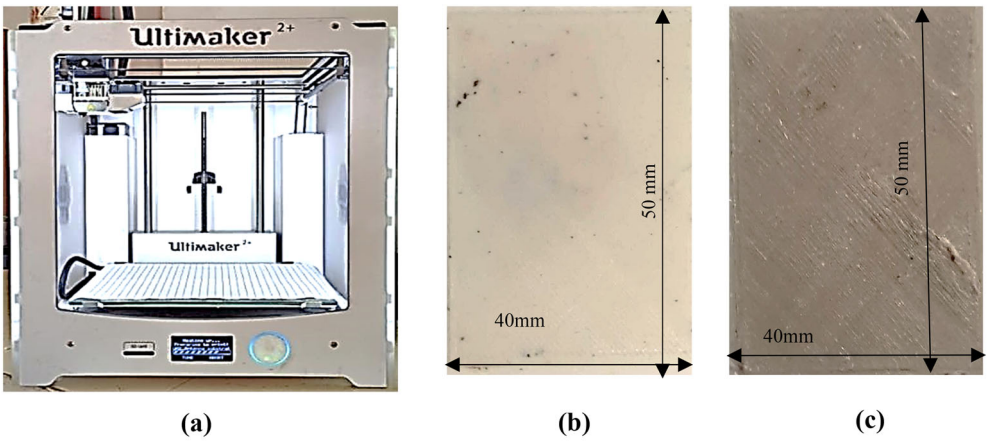

Figure 3. (**a**) Ultimaker2+ FDM setup (**b**) 3D printed 1°recycled ABS substrate (**c**) 2° recycled ABS composite substrate.

Table 3. UTM results for 1° and 2° recycled ABS composite filaments.

Composition	Peak load (N)	Break load (N)	Peak elongation (mm)	Break elongation (mm)	σ_u (MPa)	σ_f (MPa)	E (MPa)	G (MPa)
1° Recycled ABS	204.2	185.31	1.99	2.18	41.97	37.15	856.5	0.8358
2° Recycled ABS	186.1	167.78	1.89	1.47	33.55	34.77	713.8	0.7823

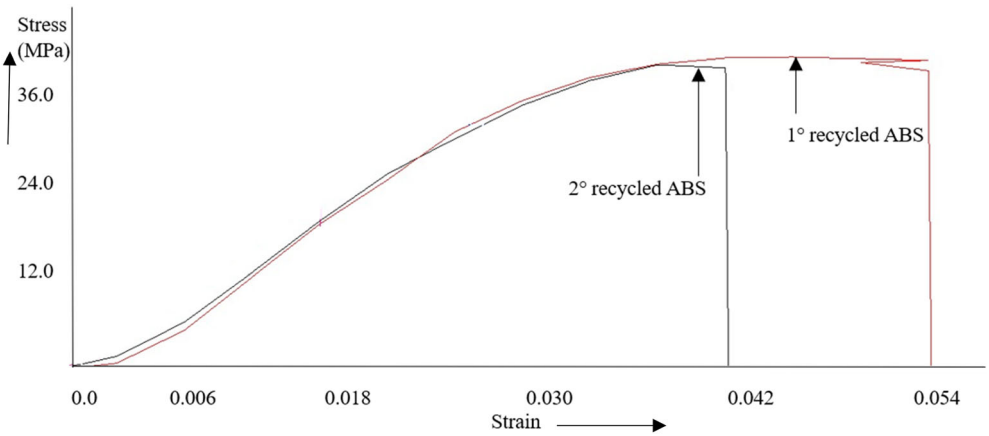

Figure 4. Stress-strain graph (as per table 3).

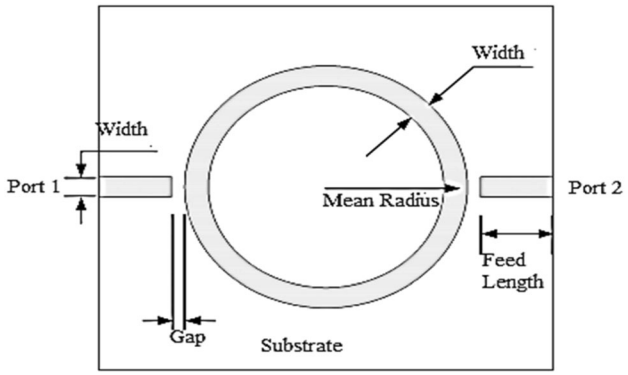

Figure 5. Schematic of a ring resonator [10].

Table 4. Dimensions of the ring resonator for ABS and ABS composite as substrate.

Parameters	Values (mm)
Mean radius	12.5
Width of the feed line	1.9
Feedline length	10.65
Coupling gap	0.9
Length of substrate	50
Width of substrate	40
Ring inner radius	13.45
Ring outer radius	11.55

electrical properties and bond characteristics was performed for selected composites. Figure 2 shows the work methodology adopted for the present study.

Based on acceptable mechanical and electrical properties, the FDM feedstock strands were prepared by twin-screw extrusion (TSE) and 3D printing of ABS and its composite substrates was performed. The dimensions of the substrate were designed using the HFSS software package and RF characteristics were obtained from VNA to ascertain the usefulness of the proposed composition/proportion for the desired health monitoring application.

3. Experimentation

3.1 *Rheological analysis: MFI testing*

Flowability of recycled ABS and different mechanical blended ABS-NH_4Cl-$ZnCl_2$ compositions/proportions for feasible 3D printing were investigated by the MFI test. The compositions weighing 50 g each were tested for MFI as per ASTM D 1238. The reinforcement of electrolytes was increased by weight % and tests were performed three times for each proportion, and average MFI was recorded. Table 1 shows the average MFI of primary (1°) and 2° recycled ABS compositions/proportions. It should be noted that an increase in electrolyte proportion, increases the probabilities of cross-linking in the ABS matrix, which may be responsible for reduced MFI. Further, the reduction in MFI of ABS composite may be due to an additional heating cycle, which the thermoplastic matrix has to withstand during 2° recycling. For commercially available open-source 3D printers, the range for MFI lies between 2 and 4 g/10 min (without any required alterations in hardware/software of the setup) [16, 18, 19, 24].

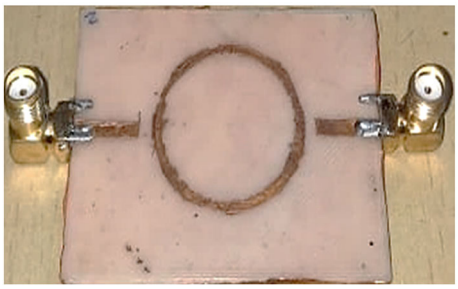

Figure 6. 3D printed ABS ring resonator samples.

3.2 *TSE*

After ascertaining the flowability of 1° and 2° recycled ABS, feedstock filaments were extruded from a commercial TSE (Make: Thermo scientific). FDM feedstock of diameter 2.75 ± 0.04 mm was obtained for ABS and 80%ABS: 10%NH_4Cl: 10%$ZnCl_2$ composite as the same were observed acceptable for 3D printing of functional parts. The temperature of extrusion was 230°C, screw speed 100 rpm along with 5 kg applied load on both compositions/proportions was fixed based upon trial runs for smooth filament fabrication (visual observation).

3.3 *Mechanical testing*

A 90 ± 0.05 mm length of 1° and 2° recycled ABS FDM spools were tested for mechanical properties by performing their tensile test on a universal tensile tester (UTT/UTM) machine as per ASTM D638. The UTM test was performed to ascertain the mechanical strength in terms of Young's modulus (E), Modulus of toughness (G), ultimate strength (σ_u), fracture strength (σ_f), etc. in the ABS and its composite for preparing durable products (useful for conformal devices and miniaturization).

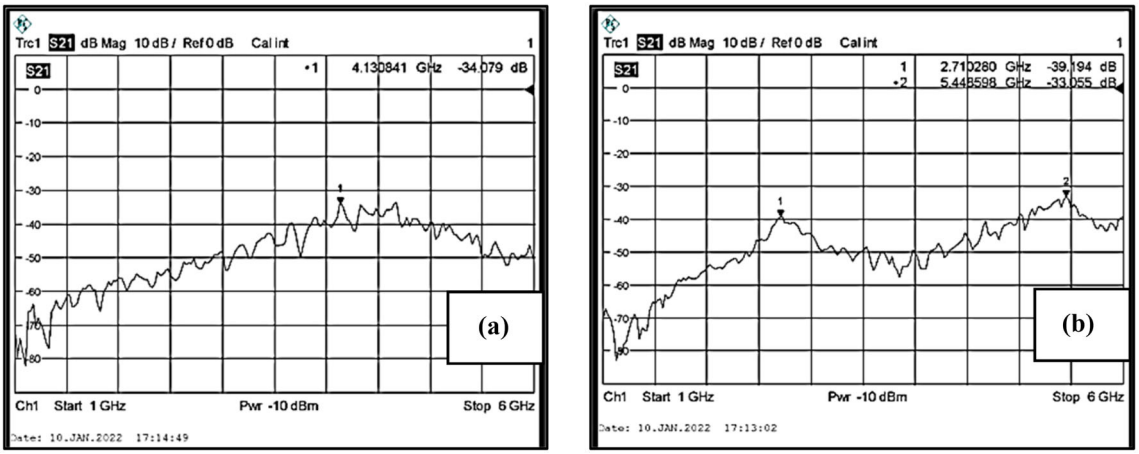

Figure 7. S_{21} parameters of ring resonator **(a)** 1° recycled ABS, **(b)** 2° recycled ABS composite.

Table 5. Calculated ε_r, and tanδ.

Substrate	Resonating frequency (GHz)		Dielectric constant (ε_r)	Loss tangent (tanδ)
	1	2		
1° Recycled ABS	4.13	–	2.8473	0.0021
2° Recycled ABS (80%ABS-10% $ZnCl_2$–10% NH_4Cl)	2.71	5.44	2.8522	0.0039

Table 6. Calculated dimensions of the patch.

Substrate	Length of a patch (mm)	Width of a patch (mm)
1° Recycled ABS	44.11	35.68
2° Recycled ABS (80%ABS-10% $ZnCl_2$–10% NH_4Cl)	44.08	35.65

3.4 *3D printing, V-I, FTIR, and RF analysis*

The V-I and FTIR-based electrical and bonding characterization of 1° and 2° recycled ABS was performed to investigate the effect of electrolytes on electrical conductivity and bond structure of 1° recycled ABS for acceptable sensor applications. Based on V-I and FTIR, the substrates of ABS and ABS-10%NH_4Cl-10%$ZnCl_2$ composite were 3D printed on an Ultimaker2+ FDM setup. The size of the 3D printed substrates was 50 × 40 × 0.75 mm. The 3D printing was performed at fixed settings: 45° raster angle, 100% infill density, infill pattern rectilinear, 03 number of the perimeter, 02 top and bottom layers. Table 2 shows the parameters selected for the FDM unit to 3D print the ABS and its composite-based substrates. Figure 3 shows the FDM setup (a), 3D printed substrate of ABS (b) and ABS-10%NH_4Cl-10%$ZnCl_2$ composite (c).

3.5 *Sensor design and simulation*

Based on the ring resonator test reported in the literature [10, 27], the RF characteristics of 3D printed ABS substrates were observed. The observations for 1° and 2° recycled ABS composite substrate were utilized in the HFSS software package to design and simulate its online health monitoring-based sensor application for 3D printable ESD reported in previous studies [24]. The morphological analysis based on SEM-EDS and area mapping was performed to investigate the effect of electrolytes on improving recyclability and industrial applications of 2° recycled ABS.

4. Results and discussion

4.1 *UTM results*

The results obtained for average mechanical properties (like E, G, σ_u, and σ_f) of 03 samples are listed in table 3. It was observed that E and G improved for 2° recycled ABS composite filament samples (figure 4). Based upon figure 4, it has been observed that in the case of 2° recycled ABS, the mechanical properties have been reduced, thus making the functional prototype a little inferior in terms of mechanical strength, but the same may be used as a sensor

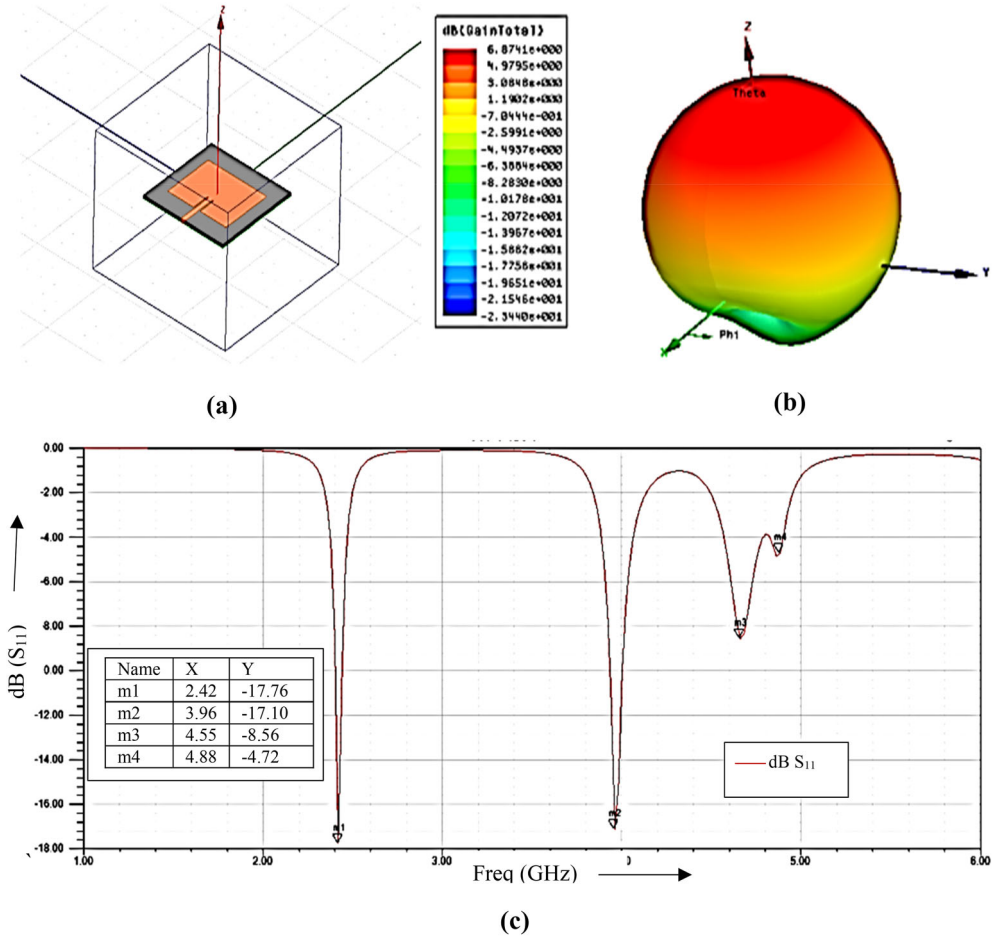

Figure 8. (**a**) 1° recycled ABS sensor design (**b**) simulated gain (**c**) simulated return loss (**d**)2° recycled ABS (**e**) simulated gain (**f**) simulated return loss.

(where mechanical strength is not the primary requirement), resulting in some value-added products.

4.2 *RF Characterization*

The ring resonator test is being used for calculating ε_r and tanδ of the thermoplastic substrate. The change in dielectric properties of the substrate may help to ascertain the health of ESD. The RF characterization was performed using the microstrip ring resonator test. A ring resonator consists of a ring-type conductor material and transmission lines on the substrate used for determining the ε_r and tanδ of any material [10, 27]. The width for the feed line has been calculated for the impedance of 50 Ω. There is a small gap between the ring and feed lines ranging from 0.1 to 1.0 times the width of the feed line [10] The basic structure of the ring resonator is shown in figure 5 [10].

The parameters used to design and analyze the patch antenna are shown in table 4.

The Cu-based conducting tape was used with a thickness of 0.08 mm. The prepared ring resonator samples are shown in figure 6.

Further, VNA was used for ascertaining the S_{21} parameters (using a range of 9 kHz to 6 GHz). It was observed that ABS resonated at 4.13 GHz with an insertion loss of −34.079 dB (figure 7a); while the ABS composite resonated at 2 peaks: 2.71 GHz (with a loss of −39.194 dB) and 5.44 GHz (with a loss of −33.055 dB) (figure 7b).

Based upon S_{21} parameters, ε_r, and tanδ were calculated [10, 27] for 1° and 2° recycled ABS (table 5).

The antenna (sensor) was designed by keeping the resonating frequency of 2.4 GHz and the 1.6 mm thickness after the required calculations [10]. The calculated dimensions of the patch are shown in table 6.

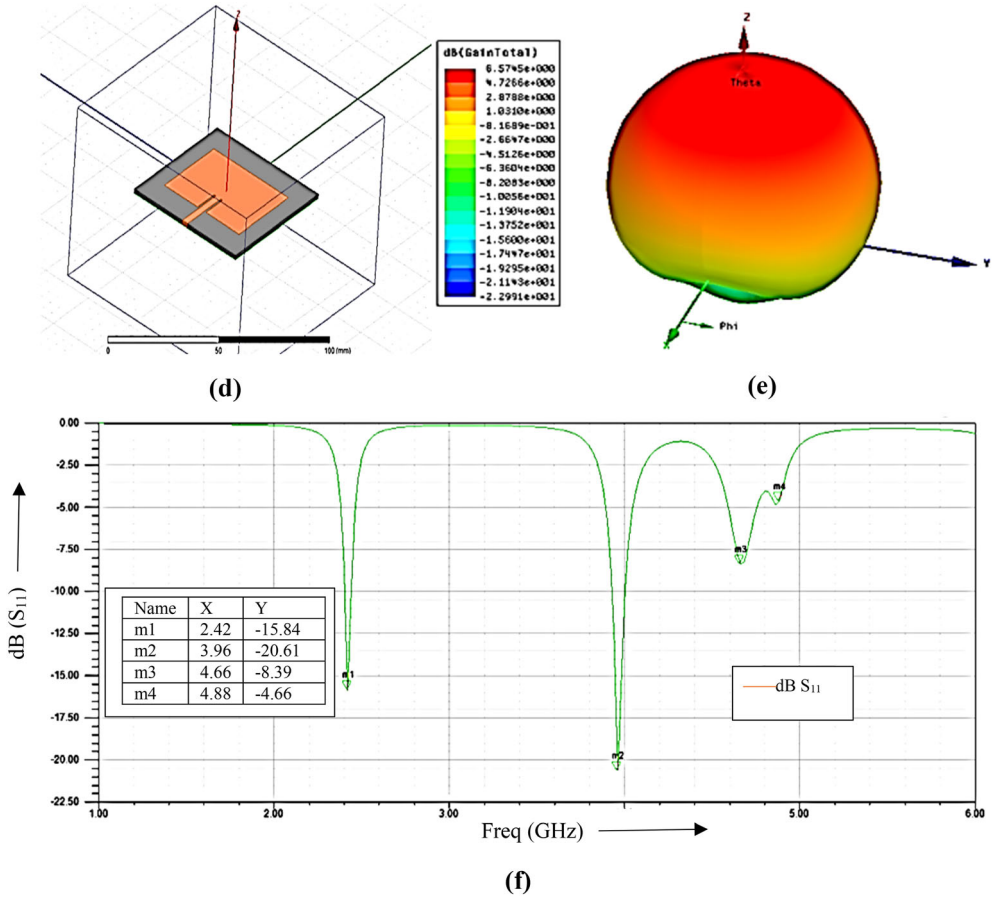

Figure 8. continued

Table 7. Simulated results.

Parameters (at 2.4 GHz)	1° Recycled ABS	2° Recycled ABS
Return loss (dB)	− 17.7615	− 15.8429
Gain (dB)	6.8741	6.5745

Table 8. V–I properties of 1° and 2° recycled ABS.

Sample	Resistance (Ω) at 1 V
1° Recycled ABS	120
2° Recycled ABS	375

The patch was designed and simulated in HFSS software for resonating at 2.4 GHz (figure 8).

Based on figure 8, the simulations show (table 7) that both the patches resonate at 2.4 GHz with the1° and 2° recycled ABS. In other words, 1°/2° recycled ABS substrate has been suitably designed to give output at 2.4 GHz and it has been observed that in the case of 2° recycled ABS the patch size was marginally reduced. The same may be calibrated to estimate the remaining life/health of ESD. These are in line with other investigators [10, 27].

4.3 *V-I characteristics*

The V-I characteristics of the samples were ascertained using Keithley 2400 Source Meter electrical tester apparatus (table 8). As observed in table 8, the resistance was significantly improved in the case of 2° recycled ABS (in line with ε_r, and tanδ, (table 5) hence may be used for sensor applications.

4.4 *Morphological analysis*

The SEM and EDS were performed on 1° and 2° recycled ABS (figure 9). In 1° recycled ABS, EDS clearly shows a

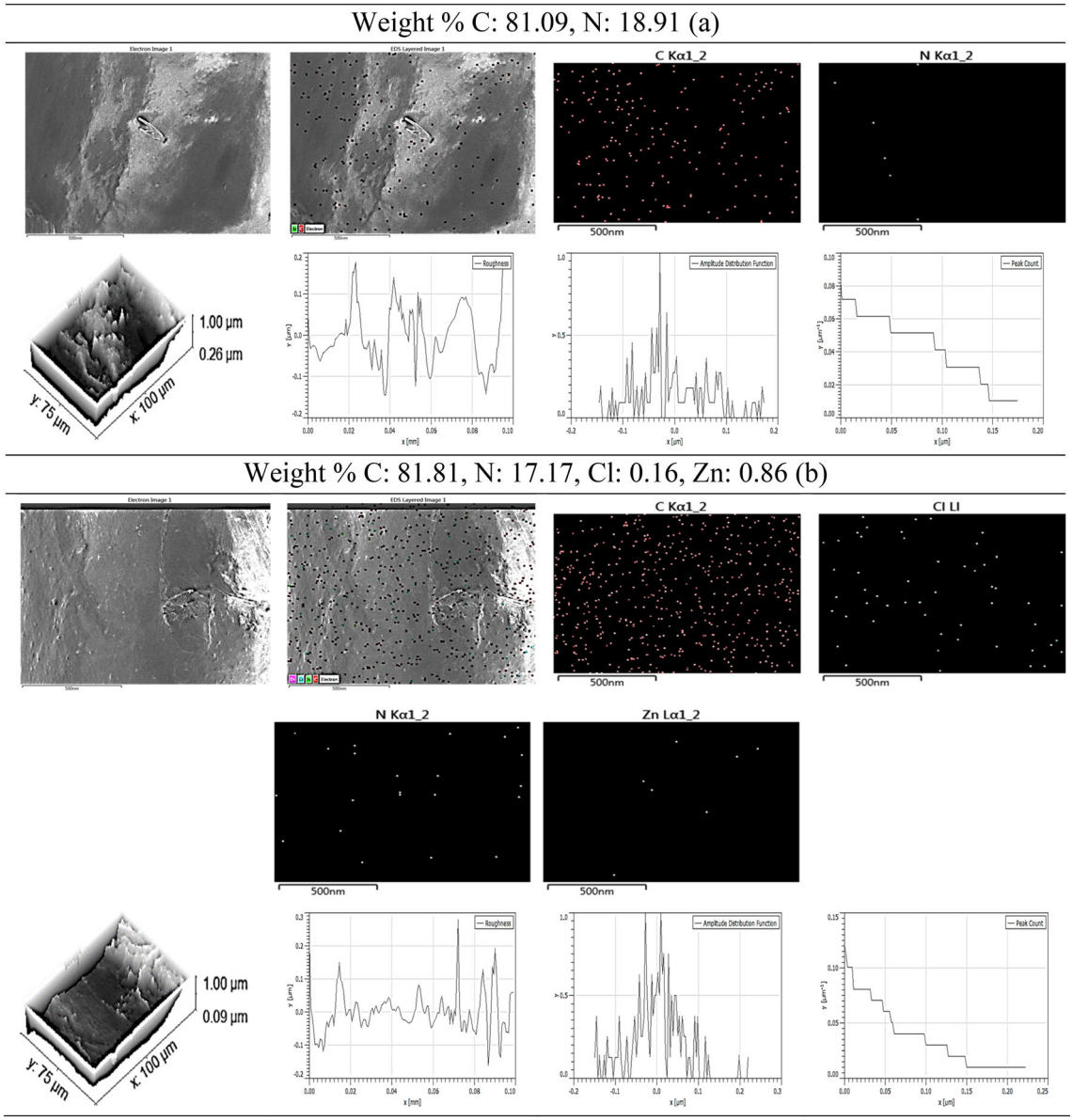

Figure 9. Surface features of (**a**) 1° recycled ABS (**b**) 2° recycled ABS.

scattering of C and N on the surface which corresponds to its chemical compositions ($C_8H_8{\cdot}C_4H_6{\cdot}C_3H_3N$) as expected (figure 9a). As observed in figure 9b traces of Zn and Cl are also available.

Further 3D rendered images, Ra profile, amplitude distribution function (ADF), and peak count (PC) were calculated based upon SEM images by using the Gwyddion open-source image processing tool (at cut-off length 0.05 mm) and Ra 25.97 µm and 28.9 µm was observed for 1° and 2° recycled ABS. The small variations in surface properties (such as the increase in Ra, ADF, and PC) in 2° recycled ABS have contributed to the change in resistance, ε_r, and tanδ of the substrate.

4.5 *FTIR analysis*

The absorbance spectrum obtained from FTIR for 1° and 2° recycled ABS compositions is shown in figure 10. The peak observed for C–H functional group at 2950 cm^{-1} wavenumber (WN) in 1° recycled ABS shifted sharply at the same WN for the 2° recycled ABS sample. At 2375WN, a sharp dip in the absorbance spectrum of ABS composite outlined the formation of a strong bond between the C≡N functional group and Cl present in the chemicals/salts. Also, the C=C bonds in 1° recycled ABS at 1489WN became strong as a shift was observed for 2° recycled ABS. The significant peak shifts for CH_2 molecules at the

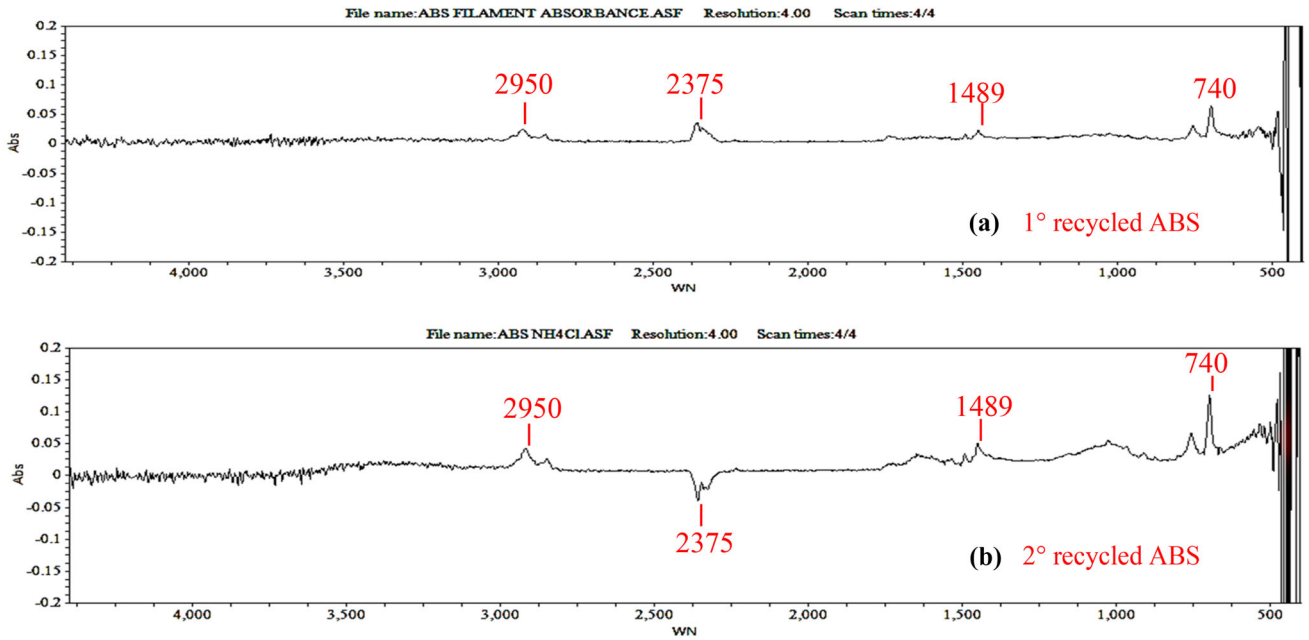

Figure 10. FTIR absorbance spectrum for(**a**)1° recycled ABS (**b**) 2° recycled ABS.

740–770 WN range also highlighted the same trend that contributed to the increase in mechanical, bonding, and electrical properties in 2° recycled ABS for sensing applications. These are in line with other investigators [19, 24, 27, 30].

5. Conclusions

Following are the conclusions from the present study:

1. Based upon the observed mechanical and electrical properties, the 3D printed sensor composed of electrolyte reinforced ABS composite may help for online condition monitoring of ESD. Hence it may contribute as a value-added functional prototype for improving the recyclability of thermoplastic waste.
2. The rheological analysis (based upon MFI) highlighted that 1° recycled ABS may be used effectively to fabricate composite-based 3D printed sensors by reinforcement of 10% $ZnCl_2$ and 10% NH_4Cl.
3. As regards mechanical, electrical, and bond structure properties are concerned, the ABS- $ZnCl_2$- NH_4Cl composite prepared by 2° recycling of ABS possesses acceptable E, G, V–I, and bond strength to impart durability to 3D printed sensor for online condition monitoring of ESD.
4. The RF properties outlined that the composite-based sensor may be calibrated to indicate the changes in the health of ESD with a variation of charge capacity in terms of ε_r, and tanδ.

Acknowledgment

The research has been partially funded under NTU-PU collaborated project and DST (GoI) provided research facilities under the FIST project (File No. SR/FST/COLLEGE/2020/997).

References

[1] Jayanth N and Senthil P 2019 Application of 3D printed ABS based conductive carbon black composite sensor in void fraction measurement. *Compos. Part B: Eng.* 159: 224–230

[2] Petroni J M, Neves M M, de Moraes N C, da Silva R A B, Ferreira V S and Lucca B G 2021 Development of highly sensitive electrochemical sensor using new graphite/acrylonitrile butadiene styrene conductive composite and 3D printing-based alternative fabrication protocol. *Anal. Chim. Acta* 1167: 338566

[3] Talukder M S, Alam M M, Islam M T, Moniruzzaman M, Azim R, Alharbi A G, Khan A I, Moinuddin M and Samsuzzaman M 2022 Rectangular slot with inner circular ring patch and partial ground plane based broadband monopole low SAR patch antenna for head imaging applications. *Chin. J. Phys.* 77: 250–268

[4] Sadasivam S, Bai V T, Yuvaraj R, Rahul P S and Thomas M R 2022 Comparison of FR4 and roger substrates in multiband two-slot rectangular patch antenna for 5G applications. *Mater. Today: Proc.* 55: 452–454

[5] Kesarwani A K, Yadav M, Singh D and Gautam G D 2022 A review on the recent applications of particle swarm

optimization and genetic algorithm during antenna design. *Mater. Today: Proc.* 56: 3823–3825

[6] Zhang Kun Da, Zhao Wei Chen, Zheng Liangang, Yao Lan, Qiu Yiping and Fujun Xu 2022 Three-dimensional woven structural glass fiber/polytetrafluoroethylene (PTFE) composite antenna with superb integrity and electromagnetic performance. *Compos. Struct.* 281: 115096

[7] Kumar R, Pandey A K, Singh R and Kumar V 2020 On nano polypyrrole and carbon nano tube reinforced PVDF for 3D printing applications: rheological, thermal, electrical, mechanical, morphological characterization. *J. Compos. Mater.* 54: 4677–4689

[8] Prakash C, Senthil P and Sathies T 2021 Fused deposition modeling fabricated PLA dielectric substrate for microstrip patch antenna. *Mater. Today: Proc.* 39: 533–537

[9] Kim D, Kim J, Kim J, Kim M, Jun O C, Park W S and Hwang W 2012 Design and fabrication of a composite-antenna-structure for broadband frequency with microwave absorber. *J. Compos. Mater.* 46: 1851–1858

[10] Singh R, Kumar S, Singh A P and Wei Y 2022 On comparison of recycled LDPE and LDPE–bakelite composite based 3D printed patch antenna. *Proc. Inst. Mech. Eng. Part L: J. Mater. Des. Appl.* 236: 842–856

[11] Tamim A M, Faruque M R and Islam M T 2021 Metamaterial-inspired electrically small antenna for microwave applications. *Proc. Inst. Mech. Eng. Part L: J. Mater. Des. Appl.*. https://doi.org/10.1177/14644207211011499

[12] MacDonald E, Espalin D, Doyle D, Muñoz J, Ambriz S, Coronel J, Williams A and Wicker R 2018 Fabricating patch antennas within complex dielectric structures through multi-process 3D printing. *J. Manuf. Process.* 34: 197–203

[13] Blaž N V, Živanov L D, Kisić M G and Menićanin A B 2022 Fully 3D printed rolled capacitor based on conductive ABS composite electrodes. *Electrochem. Commun.* 134: 107178

[14] Chen Y, Lu J, Guo Q and Wan L 2020 3D printing of CF/nylon composite mold for CF/epoxy parabolic antenna. *J. Eng. Fibers Fabr.*. https://doi.org/10.1177/1558925020969484

[15] Singh T, Kumar S and Sehgal S 2020 3D printing of engineering materials: a state of the art review. *Mater. Today: Proc.* 28: 1927–1931

[16] Kumar V, Singh R and Ahuja I P S 2022 Secondary recycled acrylonitrile–butadiene–styrene and graphene composite for 3D/4D applications: rheological, thermal, magnetometric, and mechanical analyses. *J. Thermoplast. Compos. Mater.* 35: 761–781

[17] Singh I and Tripathi V S 2011 Micro strip patch antenna and its applications: a survey. *Int. J. Comput. Technol. Appl.* 2: 1595–1599

[18] Kumar V, Singh R and Ahuja I P S 2021 On correlation of rheological, thermal, mechanical and morphological properties of chemical assisted mechanically blended ABS-Graphene composite as tertiary recycling for 3D printing applications. *Adv. Mater. Process. Technol.*. https://doi.org/10.1080/2374068X.2021.1913324

[19] Kumar V, Singh R and Ahuja I P S 2022 On 4D capabilities of chemical assisted mechanical blended ABS-nano graphene composite matrix. *Mater. Today: Proc.* 48: 952–957

[20] Ji X 2021 A perspective of ZnCl2 electrolytes: the physical and electrochemical properties. *eScience* 1: 99–107. https://doi.org/10.1016/j.esci.2021.10.004

[21] Jang J, Kim J and Bae J Y 2005 Effects of Lewis acid-type transition metal chloride additives on the thermal degradation of ABS. *Polym. Degrad. Stab.* 88(2): 324–332

[22] Zhi C, Liang Y S, Zong W C, Guo J H, Zhou J P, Mao Y J, Ji D J, Jiao P X and Yang Z P 2022 NH_4Cl promotes apoptosis and inflammation in bovine mammary epithelial cells via the circ02771/miR-194b/TGIF1 axis. *J. Integrat. Agric.* 21: 1161–1176

[23] Yang Q, Huo D, Han X, Gu C, Hou Q, Zhang F, Si C, Liu Z and Ni Y 2021 Improvement of fermentable sugar recovery and bioethanol production from eucalyptus wood chips with the combined pretreatment of NH_4Cl impregnation and refining. *Ind. Crops Prod.* 167: 113503

[24] Singh R, Singh H, Farina I, Colangelo F and Fraternali F 2019 On the additive manufacturing of an energy storage device from recycled material. *Compos. Part B: Eng.* 156: 259–265

[25] Singh R, Sandhu G S, Penna R and Farina I 2017 Investigations for thermal and electrical conductivity of ABS-graphene blended prototypes. *Materials.* 10: 881

[26] Kumar R, Singh R and Farina I 2018 On the 3D printing of recycled ABS, PLA, and HIPS thermoplastics for structural applications. *PSU Res. Rev.* 2: 115–137

[27] Jain C, Dhaliwal B S and Singh R 2022 On 3D printed ABS based sensors: rheological, mechanical, morphological, RF and 4D capabilities. *J. Mater. Eng. Perform.*. https://doi.org/10.1007/s11665-022-06884-4

[28] Singh R, Singh I and Kumar R 2019 Mechanical and morphological investigations of 3D printed recycled ABS reinforced with bakelite–SiC–Al_2O_3. *Proc. Inst. Mech. Eng. Part C: J. Mech. Eng. Sci.* 233: 5933–5944

[29] Sharma R, Singh R, Batish A and Ranjan N 2022 On synergistic effect of $BaTiO_3$ and graphene reinforcement in polyvinyl diene fluoride matrix for four-dimensional applications. *Proc. Inst. Mech. Eng. Part C: J. Mech. Eng. Sci.* 236: 276–292

[30] Singh R, Prakash S, Kumar V and Pabla B S 2022 3D printed flame retardant, ABS-$C_4H_8N_6O$ composite as energy storage device. *Arab. J. Sci. Eng.* (in-Press)